

## Supplementary Material

### 1 SUPPLEMENTARY TABLES AND FIGURES

#### 1.1 Figures

We present data that show how mechanical motions in microtubules affect the superradiant states they can support. In Figs. S1 and S2, we display visualizations of superradiant eigenstates obtained by diagonalizing the non-Hermitian Hamiltonian in Eq. 1 in the main text. Each eigenstate is near the lowest excitonic state of the system but is not necessarily the maximally superradiant state. The projection of the eigenstate onto the tryptophan (Trp) site basis gives the probabilities of each Trp being in an excited state. Either monomer chain ( $\alpha$  or  $\beta$ ) of each tubulin dimer is colored based on the average of the probability of each of the four Trp molecules in that chain being excited. Red implies a higher probability, and blue implies a lower probability. Highly superradiant states in the middle column are delocalized across the microtubule (i.e., a more uniform probability distribution), as reflected in the smaller  $P_{\max}$  values shown. (The  $P_{\min}$  values for all three columns are all numerically zero, to one part in a trillion.) Each row in Figs. S1 and S2 represents a different (mechanical) vibrational mode, which can be roughly categorized as stretching, bending, torsional, and breathing modes. The three panels in each row represent snapshots of each specific mode at different instances in time. The left and right columns display each mode at their extreme amplitudes of vibration, and the middle column displays each mode at its zero amplitude.

#### 1.2 Tables

Table S1 describes how the heatmap colors used for each panel in Figs. S1 and S2 correspond to probability distributions across each microtubule.

Mode	Left Panel		Middle Panel		Right Panel	
	$P_{\max}$	$P_{\min}$	$P_{\max}$	$P_{\min}$	$P_{\max}$	$P_{\min}$
7	0.484	$1.73 \times 10^{-17}$	0.222	$5.74 \times 10^{-15}$	0.492	$8.95 \times 10^{-16}$
8	0.414	$1.30 \times 10^{-16}$	0.109	$1.43 \times 10^{-13}$	0.424	$5.69 \times 10^{-17}$
9	0.499	$1.01 \times 10^{-14}$	0.218	$6.89 \times 10^{-14}$	0.498	$6.89 \times 10^{-16}$
10	0.483	$1.24 \times 10^{-16}$	0.261	$6.78 \times 10^{-16}$	0.478	$3.70 \times 10^{-17}$
11	0.428	$3.64 \times 10^{-16}$	0.289	$1.29 \times 10^{-14}$	0.482	$7.22 \times 10^{-16}$
12	0.499	$4.07 \times 10^{-19}$	0.290	$1.68 \times 10^{-14}$	0.499	$6.94 \times 10^{-17}$
13	0.500	$2.09 \times 10^{-16}$	0.394	$1.05 \times 10^{-15}$	0.499	$1.98 \times 10^{-17}$
14	0.500	$1.19 \times 10^{-16}$	0.261	$2.22 \times 10^{-14}$	0.500	$5.63 \times 10^{-18}$
15	0.481	$5.55 \times 10^{-17}$	0.126	$5.74 \times 10^{-14}$	0.358	$7.09 \times 10^{-14}$
16	0.500	$4.13 \times 10^{-18}$	0.395	$2.92 \times 10^{-15}$	0.500	$2.72 \times 10^{-17}$
17	0.492	$6.22 \times 10^{-17}$	0.220	$4.06 \times 10^{-15}$	0.500	$2.46 \times 10^{-17}$
18	0.498	$1.79 \times 10^{-16}$	0.303	$2.54 \times 10^{-14}$	0.490	$1.01 \times 10^{-15}$
19	0.491	$3.39 \times 10^{-16}$	0.214	$1.745 \times 10^{-15}$	0.492	$5.10 \times 10^{-16}$
20	0.491	$2.38 \times 10^{-16}$	0.194	$2.97 \times 10^{-14}$	0.496	$1.33 \times 10^{-16}$

**Table S1.** Heatmap ranges for each panel of Figs. S1 and S2.  $P_{\max}$  and  $P_{\min}$  are the maximum and minimum excitonic occupation probabilities, respectively, which range from 0 to 1.  $P_{\max}$  is associated with red,  $P_{\min}$  is associated with blue, and intermediate probabilities are associated with green in Figs. S1 and S2.

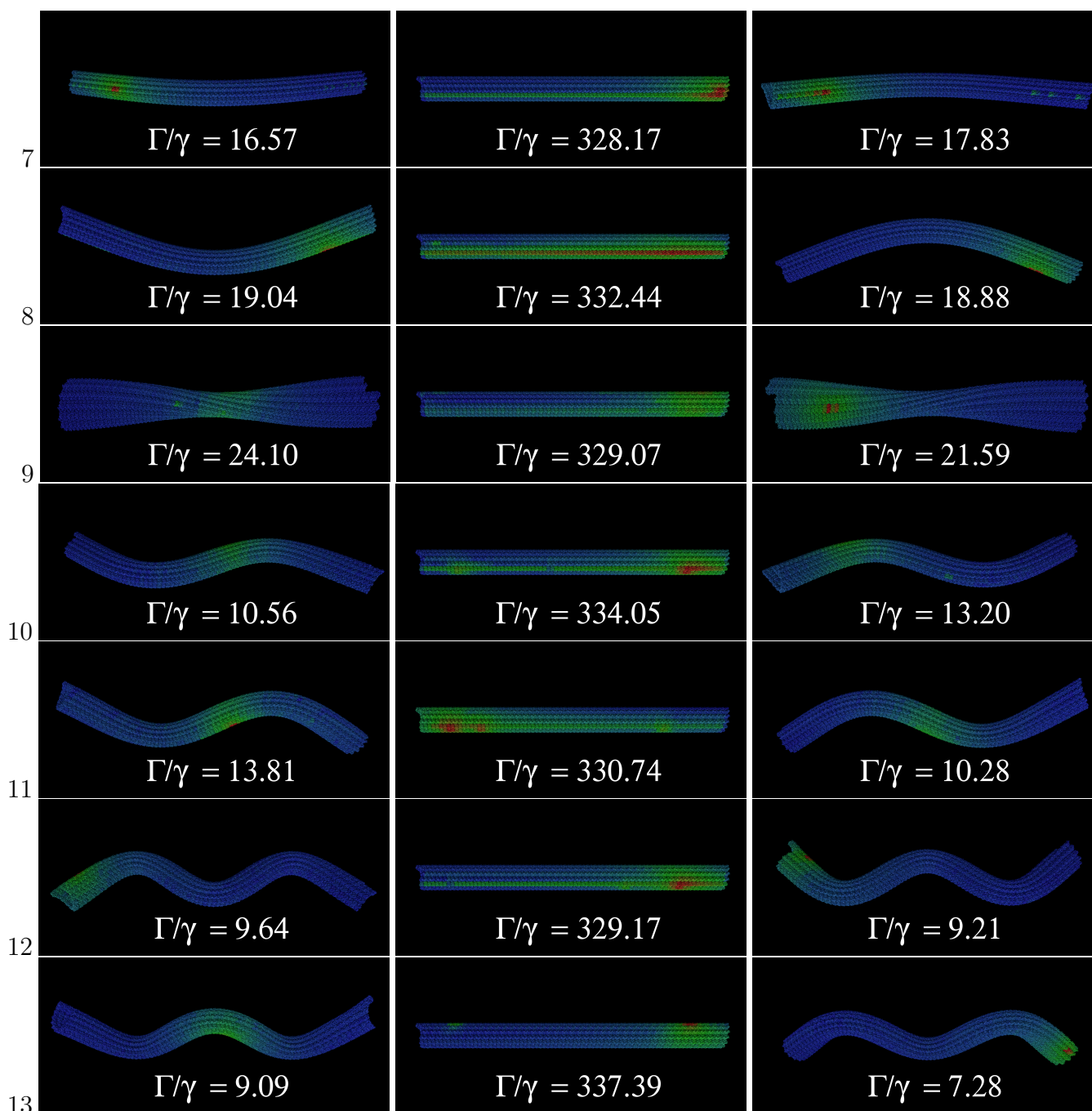


**Figure S1.** Visualizations of color-coded probability maps showing exciton occupations for low-lying excitonic energy states in the Trp site basis, labeled by maxima of superradiant enhancement factors  $\Gamma/\gamma$  of Trp networks for deformed (left and right columns) and undeformed (middle column) microtubules, realized during half a period of each mechanical mode. Atomistic simulations of vibrational motions were realized using the normal mode analyses of entire microtubules obtained from Havelka et al. (2017). Each row displays three snapshots of microtubule conformations for each of the vibrational modes 7-13 (e.g., see Fig. 3 of Havelka et al. (2017)). Rigid modes 1-6 are not shown because they do not involve deformations.

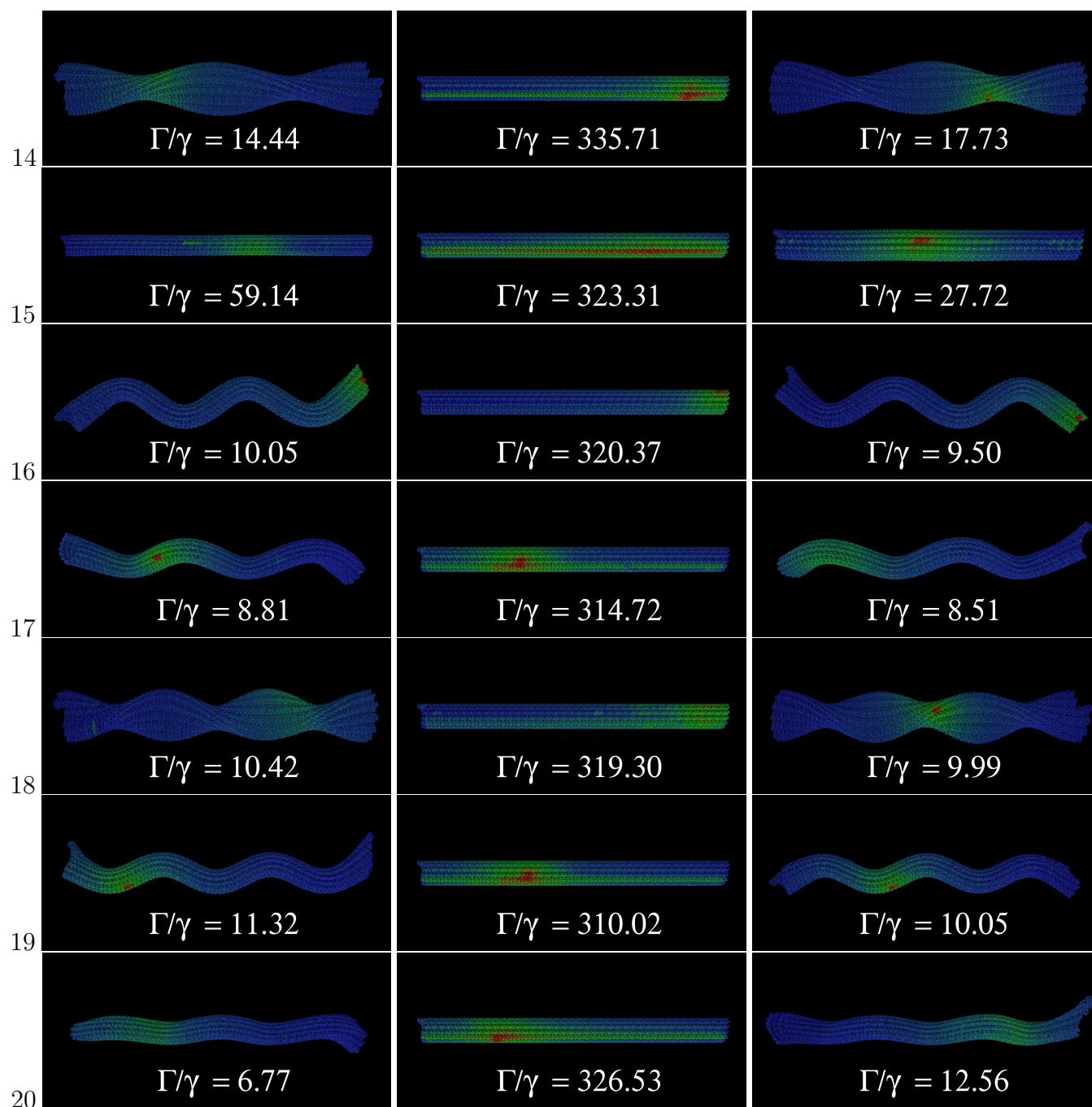


**Figure S2.** Visualizations of color-coded probability maps showing exciton occupations for low-lying excitonic energy states, labeled by maxima of superradiant enhancement factors  $\Gamma/\gamma$  of Trp networks for deformed (left and right panels) and undeformed (middle panel) microtubules. Atomistic simulations of vibrational motions were realized using the normal mode analyses of entire microtubules obtained from Havelka et al. (2017). Each row displays three snapshots of microtubule conformations for each of the vibrational modes 14-20 (e.g., see Fig. 3 of Havelka et al. (2017)).

## REFERENCES

Havelka D, Deriu MA, Cifra M, Kučera O. Deformation pattern in vibrating microtubule: Structural mechanics study based on an atomistic approach. *Scientific Reports* **7** (2017) 4227. doi:<https://doi.org/10.1038/s41598-017-04272-w>.